Diffusion of Ga adatoms at the surface of GaAs(001) $c(4 \times 4)\alpha$ and β reconstructions

Marcin Mińkowski[1,*] and Magdalena A. Załuska–Kotur[1,2,†]

[1]*Institute of Physics, Polish Academy of Sciences, Al. Lotników 32/46, 02–668 Warsaw, Poland*

[2]*Faculty of Mathematics and Natural Sciences, Card. Stefan Wyszynski University, ul Dewajtis 5, 01-815 Warsaw, Poland*

Diffusion of a Ga adatom at the As-rich, low temperature $c(4 \times 4)$ reconstructions of a GaAs(001) surface is analyzed. We use a known energy landscape for the motion of a Ga adatom at two different α and β surface phases to calculate diffusion tensor by means of the variational approach. A diffusion coefficient describes the character of low density adatom system motion at the surface. The resulting expressions allow us to identify the main paths of an adatom diffusion and to calculate an activation energy of this process. It is shown that diffusion at the α surface is slower and more anisotropic than for the β surface.

I. INTRODUCTION

Surface diffusion is a control factor of layer by layer crystal growth, one of the basic processes in the construction of nanotechnological devices. The analysis of surface diffusion is based on the determination of adsorption sites, adparticle binding energy at each of these sites, and barriers for thermally activated jumps between them. When all these parameters are calculated, the next step is to describe the particle diffusion process in this energy landscape. Development of *ab initio* calculations in the last few years resulted in a very accurate description of the surface energy landscape at various systems [1–14]. For many crystals, important because of their applications in nanotechnology or biotechnology, the full energy map at the specific surface orientations and reconstructions were done. The system which is often a subject of study is the surface GaAs(001) in its various phases such as high temperature (2×4) [15,16] or low temperature $c(4 \times 4)$ [16–27] reconstructions. This semiconductor is very important in the production of solar cells or microwave circuits used in cellular phones. In this study we use, presented in Refs. [1] and [2], results of *ab initio* calculations of the energy landscape of As-rich $c(4 \times 4)\beta$ and $c(4 \times 4)\alpha$ phases for a Ga adatom. On the basis of these data we derive a diffusion coefficient for Ga atoms and compare diffusive motion at both surface structures.

The first observations of GaAs(001) surfaces at low temperatures and at the excess of As atoms established the existence of the $c(4 \times 4)\beta$ structure [17–21] and then the asymmetric phase $c(4 \times 4)\alpha$ [20–27] was found. It is generally accepted now that the As-rich $c(4 \times 4)$ surface is divided into two phases: the $c(4 \times 4)\alpha$ phase (terminated by Ga-As dimers) which depending on the As pressure exists up to 400–550 K and the $c(4 \times 4)\beta$ phase (terminated by As-As dimers) between 400 and 770 K [16,20]. Incorporation and then diffusion of Ga atoms control the growth process in As-rich conditions. That is why detailed knowledge of the Ga adatoms diffusion is so important. The experimental study of adatom diffusion is a complex problem. Even for more popular surface reconstruction (2×4) there are not many

measurements that lead to the evaluation of the diffusion coefficient [28–30], whereas for the surfaces we study here, two types of (4×4) reconstruction, there are almost no such data. In such a situation theoretical analysis of the adatom diffusion becomes an important tool in the description of the GaAs surface dynamics. The first step is a derivation of the surface energy structure from an adatom perspective. Further study can be based on some qualitative analysis of the diffusion barriers [1,2], Monte Carlo simulation data [20,31–33], molecular dynamics process [34,35], or derivation of analytic formulas [15,33,35–38].

The analytic formulas have an advantage over other methods in that they give results as a function of temperature and of all other model parameters. We propose a variational approach that was first shown to work for a many-particle diffusion process [39–43]. Below we explain how the variational approach can be used in the calculation of the tracer diffusion coefficient, which also describes diffusion in the system of low density. For systems of low density correlations can be neglected. However, the analysis of adatom motion is still not easy because the reconstructed surface of GaAs(001) $c(4 \times 4)$ in both α and β versions contains many adsorption sites for Ga adatoms and a complicated lattice of possible jumps between them. Calculation of effective diffusion coefficients in different directions and the analysis of possible modes of particle motion is very difficult when an adatom diffuses over the surface of a complex energy landscape [36–38]. It appears that on using proper variational analysis we end up with one formula for a diffusion tensor, which then can be analyzed further. The presented approach allows for systematic study of the diffusive particle motion over the surface with a definite pattern of energies of an adatom at lattice sites and the energy barriers for jumps between them. The same procedure can be easily applied to the more complex situations like dimer or cluster diffusion [44] or diffusion in three-dimensional (3D) systems [45,46] when only an appropriate potential energy surface is calculated, providing all positions of local equilibrium sites and energy barriers for jumps.

Below we present a general method of calculation, then we show how it works in the case of the GaAs(001) surface in two different $c(4 \times 4)\beta$ and $c(4 \times 4)\alpha$ reconstructions of the surface. We show that diffusion decreases and becomes more anisotropic when β reconstruction of the surface changes to α type. Experimentally, the reentrant behavior

---

*minkowski@ifpan.edu.pl

†zalum@ifpan.edu.pl

in the high-energy electron diffraction (RHEED) oscillation during GaAs growth can be interpreted as the evidence for particle mobility change coming from the first to the second phase [20,47]. The final expressions for the diffusion coefficient allow us to identify main diffusion paths in all cases. The effective activation energy value can be calculated for the diffusion coefficient and for each diffusion path separately.

II. CALCULATION OF THE DIFFUSION COEFFICIENT

To describe the random walk of single or uncorrelated adatoms over a crystal surface we define the tracer diffusion tensor [36,48]

$$D_{n,m} = \lim_{t \to \infty} \frac{1}{4t} \langle \Delta r_n(t) \Delta r_m(t) \rangle, \qquad (1)$$

where $\Delta r_{n[m]}(t)$ is the adsorbate displacement after time t with respect to the initial position, along the coordinate $n[m] = x, y$. Definition (1) in an experimental situation corresponds to the diffusion coefficient for the adatom system of low density. The adatom diffusion which we want to describe is realized in random walk motion between different adsorption sites located at the crystal surface. To analyze this motion let us divide the lattice of the adsorption sites at the crystal surface into unit cells. We assume that each cell contains m sites located in positions $\vec{r}_j^\alpha = \vec{r}_j + \vec{a}_\alpha; \alpha = 1, \ldots, m$, where $\vec{r}_j$ describes the given cell location and $\vec{a}_\alpha$ is a location of the site within the cell. The particle at the site described by parameters (j, α) has the energy $E(\alpha)$. The equilibrium probability of finding an adatom at this site is equal to $P_{\text{eq}}(\alpha) = \rho \exp[-\beta E(\alpha)] / \sum_\gamma \exp[-\beta E(\gamma)]$, where the sum is over all sites in the unit cell, $\beta = 1/(k_B T)$ means the inverse temperature parameter, and ρ is the density of particles at the surface calculated as a number of particles divided by the number of unit cells.

The diffusion motion consists of a series of thermally activated jumps. The adsorbate in an initial adsorption state α after a given time escapes to another adsorption site γ with a transition probability per unit time $W(j, \alpha; l, \gamma)$. In order to determine the transition probabilities, we apply the transition state theory (TST) [49], according to which $W(j, \alpha; l, \gamma)$ are functions of the difference between energy barrier $\tilde{E}(j, \alpha; l, \gamma)$ for the particle jump between sites j, α and l, γ and $E(\alpha)$, the particle energy at the initial adsorption site

$$W(j, \alpha; l, \gamma) = W_{\alpha, \gamma} = \nu \exp\{-\beta [\tilde{E}(j, \alpha; l, \gamma) - E(\alpha)]\}. \qquad (2)$$

Both energies can be derived from *ab initio* calculations [1,32,50]. Proper expression for the diffusion prefactor ν is a more complex issue. Within TST approach it can be written as $\nu = k_b T Z_a / (h Z_S)$, where h is Planck's constant and Z_a, Z_S are partition functions related to the phonon modes at the adsorption well and saddle point, respectively. Now, when we calculate these functions within a harmonic approximation temperature dependence cancels out [11,35,37,38,49]. More elaborate calculations done for metallic surfaces in Ref. [51] show that ν can be constant or even weakly decreasing as a function of temperature. The phonon modes are not expected to vary much from site to site. Hence, as a first approximation

we can assume that the prefactor is site independent. Thus in our calculations below ν does not depend on temperature and has the same value for each site. We assume that $\nu = 10^{13} \text{ s}^{-1}$, close to the value of surface phonon frequencies in a GaAs crystal. This value can be easily changed in the final results, because as it is the same for each jump, it comes to be one constant that stays before the diffusion coefficient. Hence, in the following all temperature dependence of the effective activation energies and effective prefactors for the total diffusion coefficient is a result of different activation energies for individual jumps. From the other side our final formulas do not depend on the specific form of the transition probability (2), hence they allow us to use different ν values if only known.

Activation energies depend on the site from which adatom jumps and on the jump direction. Note that a particle can jump within one cell or between two different cells j and l, so energy $\tilde{E}$ depends on parameters $j, \alpha; l, \gamma$ where $l = j$ when both sites belong to the same elementary cell or $j \neq l$ when the particle changes cell on jumping. $E(\alpha)$ depends only on the type α of the site within a given cell. The structure of all possible transitions at the surface can be quite complex, especially when they happen between sites of different energy located irregularly within the cell.

The diffusion coefficient defined by (1) refers to single particle motion and we assume that our low density system is a collection of independently moving single particles. The probability that the particle occupies a given site changes with time according to the classical master equation

$$\frac{d}{dt} P(j, \alpha; t) = \sum_{l, \gamma} [W_{\gamma, \alpha} P(l, \gamma; t) - W_{\alpha, \gamma} P(j, \alpha; t)], \quad (3)$$

where $W_{\gamma, \alpha}$ describes the rates of all possible adatom jumps over the lattice and fulfills the detailed balance condition

$$W_{\gamma, \alpha} P_{\text{eq}}(\gamma) = W_{\alpha, \gamma} P_{\text{eq}}(\alpha). \qquad (4)$$

All components W can be gathered in one matrix $\hat{W}$ with elements $-\sum_{l, \gamma} W_{\alpha, \gamma}$ at the diagonal location $(j, \alpha; j, \alpha)$ and $W_{\gamma, \alpha}$ out of the diagonal.

In order to analyze the character of particle diffusion it is convenient to make a Fourier transform of the master equation (3) based on the fact that an infinite surface over which the particle is wandering consists of periodically repeated cells. In the wave vector $\vec{k}$ space the vector describing the probability of the site occupation has components $P_\alpha(\vec{k}; t) = \sum_j \exp(i \vec{k} \vec{r}_j^\alpha) P(j, \alpha; t)$. Each component α of this vector corresponds to one of the sites within the unit cell. We now have m equations for m different components of the occupation probability vector

$$\frac{d}{dt} P_\alpha(\vec{k}; t) = \sum_{\gamma \neq \alpha} M(\gamma; \alpha) P_\gamma(\vec{k}; t) + M(\alpha; \alpha) P_\alpha(\vec{k}; t). \quad (5)$$

Matrix $\hat{M}$ is created from matrix $\hat{W}$ after transformation into k space which gives

$$M(\alpha; \alpha) = -\sum_{l, \gamma \neq \alpha} W_{\alpha, \gamma}, \quad M(\gamma; \alpha) = W_{\gamma, \alpha} e^{i \vec{k}(\vec{r}_l^\gamma - \vec{r}_j^\alpha)}, \quad (6)$$

where formulas are written for one, arbitrary cell j and summation goes over all sites within this cell and over all neighboring cells l. Note that off-diagonal elements $M(\gamma; \alpha)$ are $\vec{k}$ dependent.

To solve the set of Eq. (5) we should find m eigenvalues and eigenvectors of matrix $\hat{M}$. Each eigenvalue describes one dynamical mode responsible for the relaxation of the initial occupation probability towards equilibrium values. The diffusion tensor (1) can be obtained from the one particular eigenvalue of the transition rate matrix (6). It can be demonstrated [36,39,52] that for the master equation (5) there is one and only one eigenvalue $\lambda_D(\vec{k})$ such that $\lim_{|\vec{k}| \to 0} \lambda_D(\vec{k}) = 0$ and the real part of all the other eigenvalues is negative. This particular eigenvalue λ_D is a diffusional eigenvalue, which means that it is proportional to $\vec{k}^2$ and can be expressed as

$$\lim_{|\vec{k}| \to 0} \lambda_D = \lim_{|\vec{k}| \to 0} \frac{\vec{w} \hat{M} \vec{v}}{\vec{w} \vec{v}} = -\vec{k} \hat{D} \vec{k}, \qquad (7)$$

where $\vec{w}$ is the left eigenvector and $\vec{v}$ is the right one. The matrix $\hat{M}$ is not Hermitian but its elements are related to each other by the rule $M^*(\gamma; \alpha) P_{eq}(\gamma) = M(\alpha; \gamma) P_{eq}(\alpha)$ resulting from the local equilibrium balance (4). As a result eigenvectors of matrix $\hat{M}$ are connected by relation $w_\alpha^* P_{eq}(\alpha) = v_\alpha$. Equation (7) is our main formula used to derive the diffusion matrix $\hat{D}$ (1). On inserting explicit expressions (6) into (7) and taking into account normalization

$$\sum_\alpha w_\alpha v_\alpha = \sum_\alpha w_\alpha w_\alpha^* P_{eq}(\alpha) = \rho \qquad (8)$$

we can write

$$\vec{k} \hat{D} \vec{k} = \frac{1}{\rho} \lim_{|\vec{k}| \to 0} \sum_{\alpha, \gamma} w_\gamma M(\alpha, \gamma) v_\alpha$$

$$= \frac{1}{\rho} \lim_{|\vec{k}| \to 0} \sum_{\alpha, \gamma} \left(w_\alpha - e^{i\vec{k}(\vec{r}_l^\gamma - \vec{r}_j^\alpha)} w_\gamma \right) W_{\alpha, \gamma} v_\alpha. \qquad (9)$$

And when consequences of detailed balance for $M(\alpha, \gamma)$ and eigenvectors $\vec{w}, \vec{v}$ are taken into account we have

$$\vec{k} \hat{D} \vec{k} = \frac{1}{\rho} \lim_{|\vec{k}| \to 0} \left[\sum_{\alpha > \gamma} \left(w_\alpha - e^{i\vec{k}(\vec{r}_l^\gamma - \vec{r}_j^\alpha)} w_\gamma \right) W_{\alpha, \gamma} P_{eq}(\alpha) w_\alpha^* \right.$$

$$\left. + \left(e^{i\vec{k}(\vec{r}_l^\gamma - \vec{r}_j^\alpha)} w_\gamma - w_\alpha \right) W_{\alpha, \gamma} P_{eq}(\alpha) w_\gamma^* e^{-i\vec{k}(\vec{r}_l^\gamma - \vec{r}_j^\alpha)} \right]$$

$$= \frac{1}{\rho} \lim_{|\vec{k}| \to 0} \sum_{\alpha > \gamma} \left| w_\alpha - e^{i\vec{k}(\vec{r}_l^\gamma - \vec{r}_j^\alpha)} w_\gamma \right|^2 W_{\alpha, \gamma} P_{eq}(\alpha). \qquad (10)$$

Our diffusional eigenvalue λ_D in the limit of small $\vec{k}$ is proportional to $\vec{k}^2$ and has the lowest absolute value of all eigenvalues. It can be found by the variational method by assuming a properly parametrized eigenvector. We choose

$$v_\alpha = P_{eq}(\alpha) e^{i\vec{k} \vec{\phi}_\alpha}, \quad w_\alpha = e^{-i\vec{k} \vec{\phi}_\alpha}. \qquad (11)$$

The above form of eigenvectors provides proper normalization and introduces variational parameters $\vec{\phi}_\alpha$ that are coupled to wave vector $\vec{k}$ so they can influence the diffusion coefficient. A similar choice of variational parameters was shown to be a good one in the description of collective diffusion at nonhomogeneous surfaces in Refs. [40–43].

On using explicit expression for eigenvectors (11) in Eq. (10) we obtain a variational formula for the diffusion coefficient $\hat{D}_{var}$,

$$\vec{k} \hat{D}_{var} \vec{k} = \lim_{|\vec{k}| \to 0} \sum_{\alpha > \gamma} W_{\alpha, \gamma} P_{eq}(\alpha) \left| e^{i\vec{k} \vec{\phi}_\alpha} - e^{\vec{k}(\vec{r}_l^\gamma - \vec{r}_j^\alpha + \vec{\phi}_\gamma)} \right|^2$$

$$= \sum_{\alpha > \gamma} W_{\alpha, \gamma} P_{eq}(\alpha) \left[\vec{k} \left(\vec{\phi}_\gamma + \vec{r}_l^\gamma - \vec{r}_j^\alpha - \vec{\phi}_\alpha \right) \right]^2. \qquad (12)$$

Now, for the final expression for $\hat{D}_{var}$ we should minimize the above equation with respect to all independent parameters $\vec{\phi}_\alpha$. Each separate type of the surface site α has its individual vector of phases, so all together we have two times more phases than sites in the elementary cage. However, one of the vector parameters $\vec{\phi}$ can be set to $\vec{0}$, because as it can be seen in (12) only phase differences count, which means that we can move all phases by the same quantity without changing the result. Moreover, phases for some sites are identical due to the system symmetry. In such a way the number of parameters can be reduced and as a result the problem is simplified. In the following sections we will show how the procedure works in practice for studying diffusion of Ga adatoms over the GaAs(001) $c(4 \times 4)$ surface.

III. DIFFUSION COEFFICIENT FOR THE Ga ADATOM AT THE GaAs(001) $c(4 \times 4)\beta$ RECONSTRUCTION

Systematic study of energies of a Ga atom at binding sites of GaAs(001) $c(4 \times 4)\beta$ surface reconstruction and of barriers for diffusion between them have been shown in Ref. [32]. Lately, a more detailed map of the surface energy was presented in Ref. [1]. We used the energy pattern calculated in this last article as a basis to the analysis of the diffusion behavior of an adsorbed Ga atom.

The scheme of the lattice for Ga adsorption sites at the GaAs(001) $c(4 \times 4)\beta$ surface is shown in Fig. 1 with numeration from Ref. [1]. When the Ga atom was relaxed from
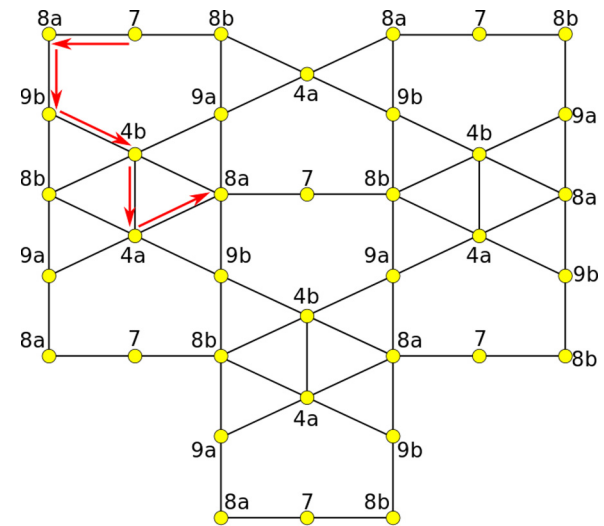

FIG. 1. (Color online) Binding sites of Ga atoms at the GaAs(001) $c(4 \times 4)\beta$ surface. Site placement and numeration on the base of Ref. [1].
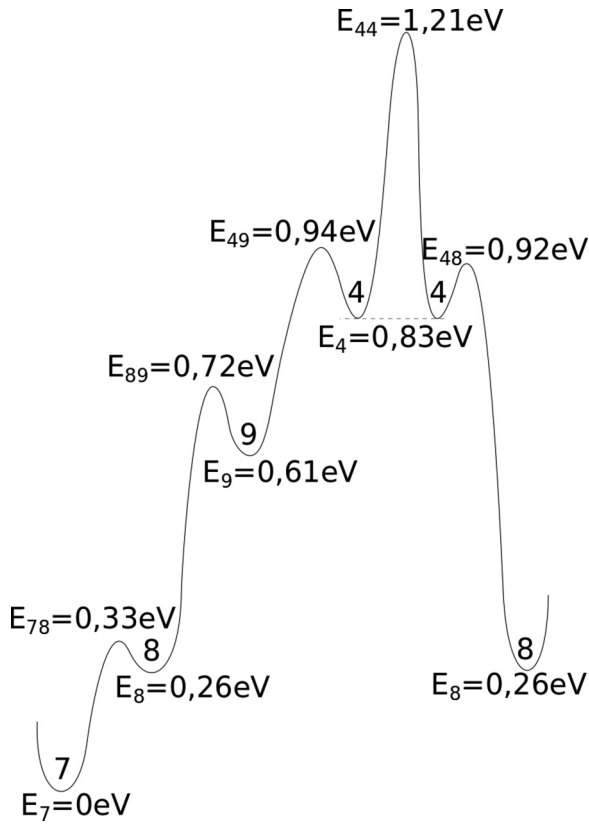
FIG. 2. Energy landscape cross section along the marked path in Fig. 1. It contains all the possible Ga adatom jumps at the surface. Energy data from Ref. [1].

3 Å above the surface seven different types of minimum energy sites were found. The lowest one with number 7 (described also as 6 [1]) lies in the trench between As dimers at the reconstructed surface and so do four other sites: 8a,8b and 9a,9b. As it was shown in Ref. [1] position and depth of the adsorption sites at hills of As dimers depends on the height from which the Ga atom is relaxed. However, if we stay at a height of 3 Å, the surface is not deformed and there is only one additional adsorption site at the surface in two versions 4a and 4b. With the same numbers and different letters we marked sites of the same depth and the same jump rates out of the site, however with different space orientation, rotated or reflected like in the cases of 8a and 8b (see Fig. 1). All energies that decide about jump rates between our sites can be presented along the path marked in Fig. 1 and the energy landscape along this path is shown in Fig. 2. It can be seen that the site of the lowest energy is 7 and there are four different adsorption site energy values at this surface. All together there are seven sites—one of energy E_7, and two types of energies E_4, E_8, and E_9 in one elementary cage.

Calculated energy barriers determine the probability of each single particle jump. An analysis of barrier heights allows us to find the easiest jump path, which has been done in Ref. [1]. However, when we look for the path with minimal energy barriers, it does not necessarily reflect the possible diffusional behavior of a single particle. When the particle moves randomly in the potential landscape like this in

Figs. 1 and 2 it jumps forward and backward with frequency proportional to the jump rate. As it can be seen when the particle jumps down, into the site of lower energy, its return is more difficult due to a higher energy barrier. It means that not only transition rates of jumps but also site occupation probabilities at equilibrium should be important in the long distance diffusive motion. Our formula (12) contains all transition rates as well as equilibrium occupation probabilities for all possible sites. The diffusion coefficient matrix describes long distance particle diffusion at equilibrium conditions. Below we calculate a tensor of diffusion coefficients for single particle motion by using the variational approach. Then we compare diffusion in different directions and finally identify dominant diffusion paths. As we will see only some of them agree with the paths of minimal energy barriers.

In Fig. 1 we plot all transitions between sites that are taken into account in the calculations below. Energy barriers for these transitions were taken from Ref. [1]. There is one more possible transition path not shown in Fig. 1 but calculated in Ref. [1]. It is the path directly from site 7 through low lying site 5 to site 4 with the activation energy as high as 1.10 eV. In comparison with other energy barriers for jumps in the systems this transition rate can be neglected at experimentally achieved temperatures. As a result there is also no need to consider any additional sites, like 5, hence we end up with four different energies of adsorption sites.

According to the rules of statistical mechanics equilibrium probability at given site is

$$P_{\text{eq}}^\alpha = \frac{\rho e^{-\beta E_\alpha}}{2e^{-\beta E_4} + e^{-\beta E_7} + 2e^{-\beta E_8} + 2e^{-\beta E_9}} \quad (13)$$

when the site occupation is normalized within elementary cage $\sum_\alpha P_{\text{eq}}^\alpha = \rho$. Equilibrium probabilities (13) should be then put into the variational formula (12) for the diffusion matrix. In general there are two variational parameters ϕ_x^α and ϕ_y^α per each site type—one coupled to the direction k_x and the other to k_y. The lattice has reflection symmetry with respect to the directions x and y and according to this symmetry $\phi_{x,y}^{9a} = -\phi_{x,y}^{9b}$—closest bonds are inverted in both directions, whereas $\phi_x^{8a} = -\phi_x^{8b}$, $\phi_y^{8a} = \phi_y^{8b}$ and inversely for site 4, $\phi_x^{4a} = \phi_x^{4b}$, $\phi_y^{4a} = -\phi_y^{4b}$. As mentioned before phases at one of the sites can be set freely, so the number of parameters is reduced to six. Axes x and y are the main directions of the diffusional tensor $\hat{D}$ for the lattice with the described symmetry, hence only diagonal parameters $D_{xx} = D_x$ and $D_{yy} = D_y$ are nonzero and each value at the diagonal depends only on parameters coupled to the corresponding direction. Finally, the following values of diffusion coefficients were found:

$$D_x^\beta = 2\left[\frac{(W_{87}W_{89} + 4W_{84}W_{87} + 2W_{84}W_{89})P_{\text{eq}}^8}{2W_{84} + W_{87} + 2W_{89}}\right. $$
$$\left. + W_{49}P_{\text{eq}}^4\right]a^2, \quad (14)$$

$$D_y^\beta = 2\left[W_{89}P_{\text{eq}}^8 + \frac{W_{49}(W_{44} + W_{48})P_{\text{eq}}^4}{W_{44} + W_{48} + W_{49}}\right]a^2, \quad (15)$$
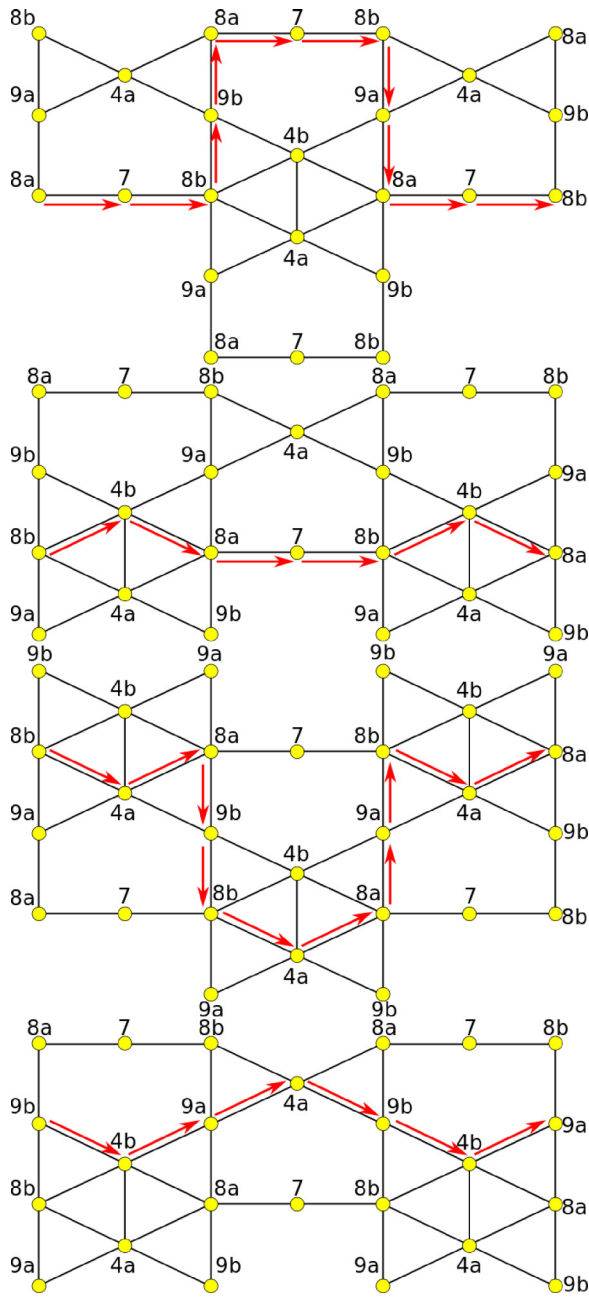
FIG. 3. (Color online) Diffusion Ga adatom paths along the x direction at the GaAs(001) $c(4 \times 4)\beta$ surface.

where $W_{\alpha,\beta}$ is given by Eq. (2) and appropriate energies can be found in Fig. 2. Lattice unitary length $a = 5.6$ Å.

In the above expressions each of the terms can be understood as a contribution of a certain path to the total diffusion. Let us note that among all paths only one in direction x (between sites 4 and 9) and one in direction y (between sites 8 and 9) are independent from the other ways of diffusion. The remaining transition rates of Eqs. (14) and (15) are all connected in one component. The numerator of both these expression is a sum of separate terms. For example, in Eq. (14) we can write the first component as a sum of three terms, each of them containing two different rates in the numerator and the same rates in the denominator plus an additional third
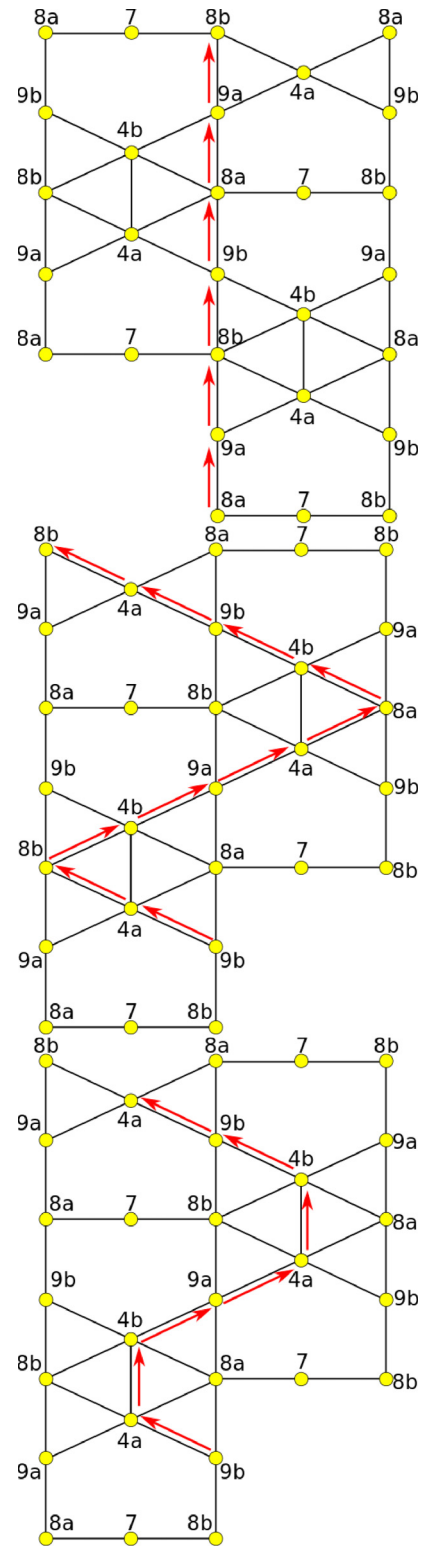

FIG. 4. (Color online) Diffusion Ga adatom paths along the y direction at the GaAs(001) $c(4 \times 4)\beta$ surface.

one. Thus we can say that each of these terms represents a path which goes through the main two links and is slightly modified by the presence of the other ways of diffusion. We can now plot all possible ways of diffusion. There are four
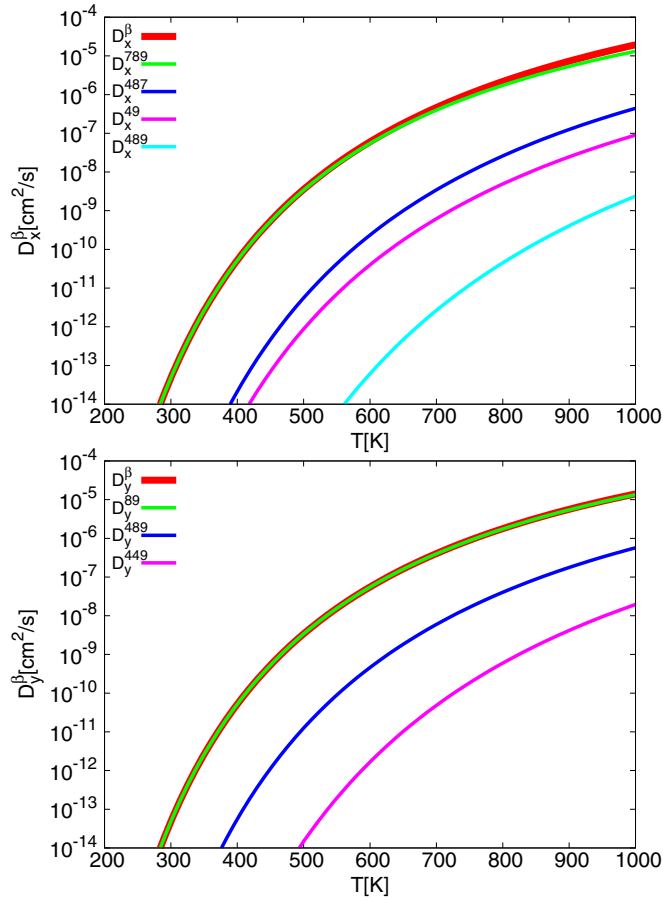
FIG. 5. (Color online) Dependence of the diffusion coefficients D_x and D_y on the temperature for the Ga atom at the GaAs(001) $c(4 \times 4)\beta$ surface.

FIG. 6. (Color online) Comparison of the diffusion coefficients D_x^β and D_y^β as a temperature function in logarithmic scale. The scale of the anisotropy coefficient is shown on the right.

paths in the x direction and three paths in the y direction. We show them in Figs. 3 and 4.

At first let us analyze diffusion along direction x. The first plotted path contains only W_{87} and W_{89} transition rates and it is the same path as was identified as the one with the lowest activation energies for jumps in Ref. [1]. In Fig. 5 we plotted the temperature dependence of a total diffusion coefficient in both directions and the contribution to this value of each identified path. Our results confirm that the path found in Ref. [1] is the most important for a large temperature range. The next important path for the diffusion coefficient is the one that goes through the hill site 4. Diffusion along this path becomes larger than the first one at higher temperatures. As explained above these paths are not entirely independent, they are linked by the denominator in one expression. This expression also contains the third path, which has the lowest diffusion values. The independent path (49) is not the fastest one, but it is interesting because it bypasses site 7, the one of the lowest energy, which means that once the particle comes out of the lowest energy site it can slide over states with higher energy. Such an independent path and avoiding site 7 is the most important one in direction y. It appears that due to the symmetry of the lattice all possible paths along direction y bypass the lowest site as can be seen in Fig. 4. However, according to plots in Fig. 5 only one path has significant effect on the overall diffusion in direction y.
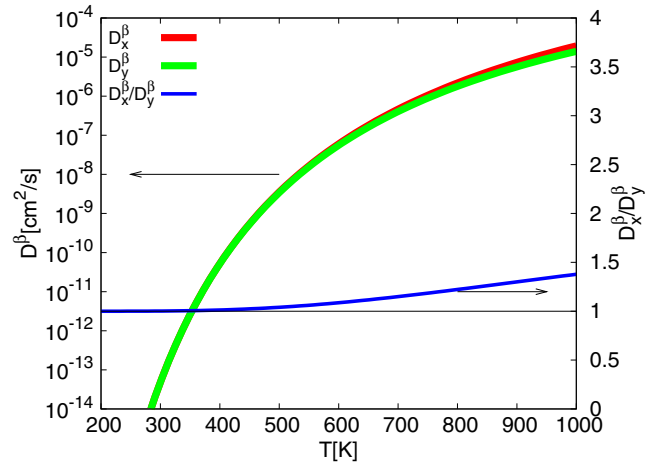
It is interesting to compare diffusion along the x and y directions. Components in both directions are plotted in Fig. 6. It can be seen that diffusion in the x direction is faster than that in direction y. Note that this difference seems to be small only due to the logarithmic scale used in this figure. In the same figure ratio between D_x and D_y is plotted in linear scale. For low temperatures the ratio is close to one, i.e., in Fig. 6 it is close to a thin horizontal line at this level. This agrees with Monte Carlo simulations in Ref. [32] where diffusion at temperature 470 K was found to be isotropic. However, at higher temperatures diffusion becomes an anisotropic process with D_x almost two times higher than D_y.

When we ignore in (14) and (15) all contributions from sites located at the dipole structure we have expressions

$$D_x = 2 \frac{W_{87} W_{89} P_{eq}^8}{W_{87} + 2W_{89}} a^2, \quad D_y = 2W_{89} P_{eq}^8 a^2, \quad (16)$$

which can be explicitly used to reproduce Monte Carlo (MC) data from Ref. [32]. When we put into the above formulas the exact energy barriers that were used in Ref. [32] we get $D_x = 1.857 \times 10^{-8}$ cm^2/s and $D_y = 1.859 \times 10^{-8}$ cm^2/s comparing with MC results 1.74×10^{-8} cm^2/s in direction x and 1.66×10^{-8} cm^2/s in direction y.

In order to analyze the diffusion process more precisely we use parametrization

$$D_x = \nu_x e^{-\beta E_A^x}, \quad D_y = \nu_y e^{-\beta E_A^y}, \quad (17)$$

where both activation energy E_A and prefactor ν can weakly depend on temperature. We calculate activation energies by using the formula

$$E_A = -\frac{\partial \ln D}{\partial \beta}. \quad (18)$$

In Fig. 7 we plot the temperature dependence of activation energies for both coefficients D_x and D_y. It can be seen that the activation energy does not change much within the range of temperature, which is important in the experiment. In both directions it starts with the same value 0.72 eV then E_A^x slightly goes up, has its maximum at 1000 K, and then decreases,
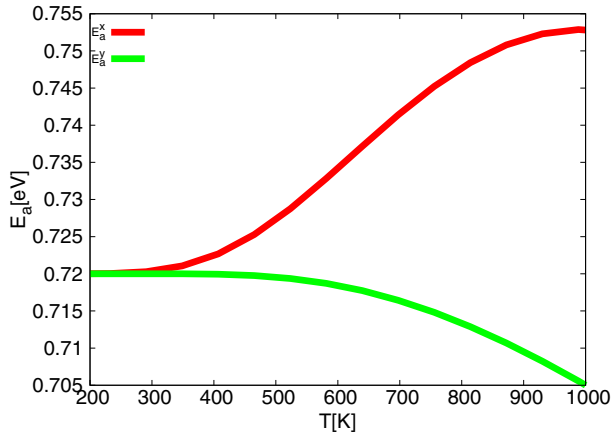
FIG. 7. (Color online) Temperature dependence of the activation energies calculated with use of (18) for total diffusion coefficients D^β in both directions.
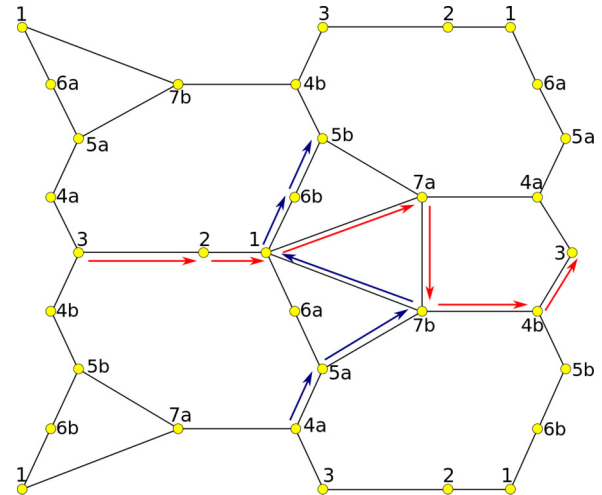

FIG. 8. (Color online) Binding sites of Ga atoms at the GaAs(001) $c(4 \times 4)\alpha$ surface. Site placement and numeration according to Ref. [2].

whereas E_A^y goes down within the presented temperature range. It is interesting that even if D_y is lower than D_x, the effective activation energy responsible for this direction is also lower that E_A^x. It means that this is not an activation energy but a prefactor ν that decides the observed anisotropy. Looking at curves in Fig. 5 it is easy to understand that diffusion in the x direction is dictated by the (789) direction at lower temperatures and then it is more and more dependent on the second channel (487), whereas diffusion along the y direction is given almost totally by one, dominant component (89). The number of important diffusion paths contributes to the prefactor, thus compensating the effect from the activation barrier difference.

We can see that at the surface with several adsorption sites and a complicated lattice of transitions a few of the most important paths can be identified. In close to equilibrium conditions particles diffuse along these paths. We have shown that the activation energy that characterizes the given diffusion path is not a simple sum of energy barriers for individual jumps between successive adsorption sites. The equilibrium diffusion coefficient strongly depends on the occupation probabilities that always accompany corresponding transition rates. However, the slowest jump in a row is the one that decides the value of the diffusion coefficient. Such property can be seen in the shape of our formulas, where sums of the reciprocals of successive rates are present. Moreover, the diffusion process does not necessarily happen through the lowest adsorption site, like our (89) path for diffusion along the y direction.

IV. DIFFUSION COEFFICIENT FOR Ga ADATOM AT GaAs(001) $c(4 \times 4)\alpha$ RECONSTRUCTION

Let us take into regard $c(4 \times 4)\alpha$ reconstruction of the same GaAs(001) surface [2,24]. The unit cell at this surface is similar to this in the β reconstruction, but with slightly different positions of atoms at the top layer. As a result adsorption sites have completely different locations and energies [2]. Thus the symmetry of the energy landscape for the Ga adatom is changed as can be seen in Fig. 8. Note that we now have 11 different adsorption sites out of which nine (1, 2, 3, 4a, 4b,
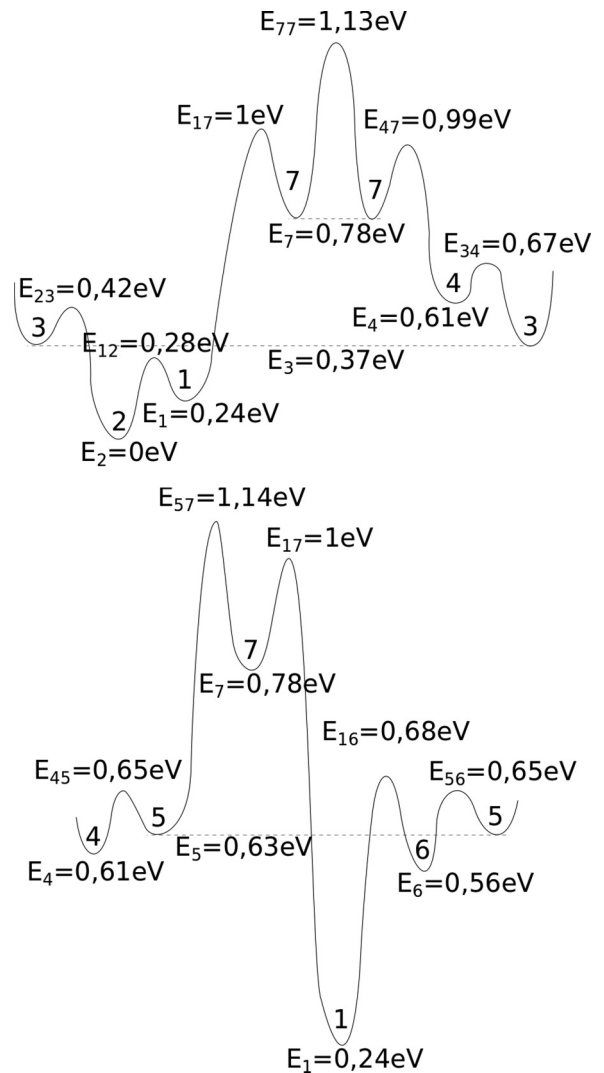

FIG. 9. Energy landscape along the marked paths in Fig. 8. They contain all the possible jumps of the Ga adatom at the surface. Energy data from Ref. [2].
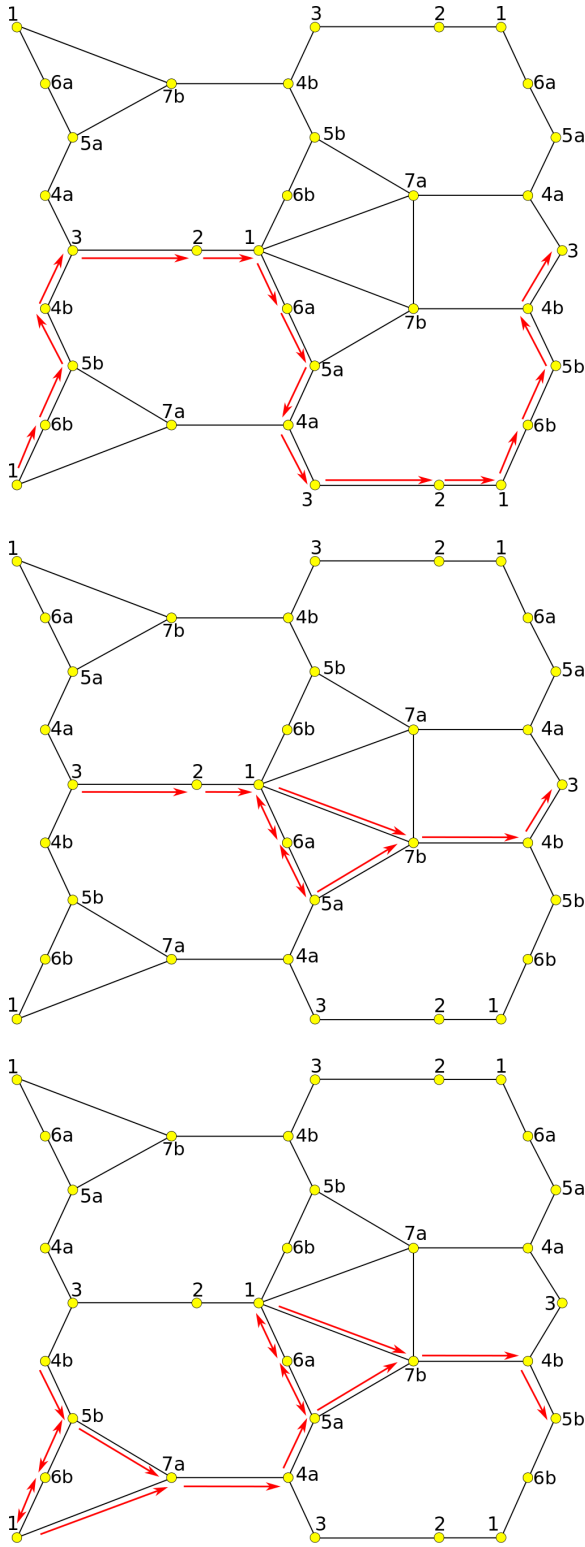
FIG. 10. (Color online) Different Ga adatom diffusion paths in direction x over the GaAs(001) $(4 \times 4)\alpha$ reconstructed surface.

5a, 5b, 6a, 6b) lie within trenches and two, namely 7a and 7b, at dimer hills. The lattice has inverse symmetry only with respect to the axis x. There is no symmetry in the perpendicular direction. The cross section of the potential energy landscape along the two paths marked in Fig. 8 is presented in Fig. 9.
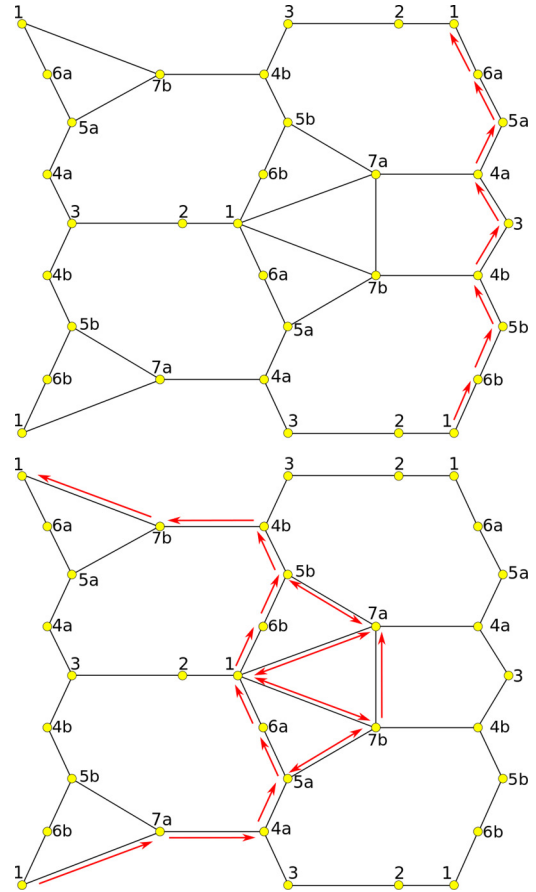

FIG. 11. (Color online) Possible Ga adatom diffusion paths in direction y over the GaAs(001) $(4 \times 4)\alpha$ reconstructed surface.

Our calculations of the diffusion coefficient start with formulas for equilibrium probabilities:

$$P_{\text{eq}}^{\alpha} = \frac{\rho e^{-\beta E_\alpha}}{\sum_{i=1}^{7} e^{-\beta E_i}}. \tag{19}$$

Variational vector (11) is constructed with two independent phases for each lattice site. According to the lattice symmetry
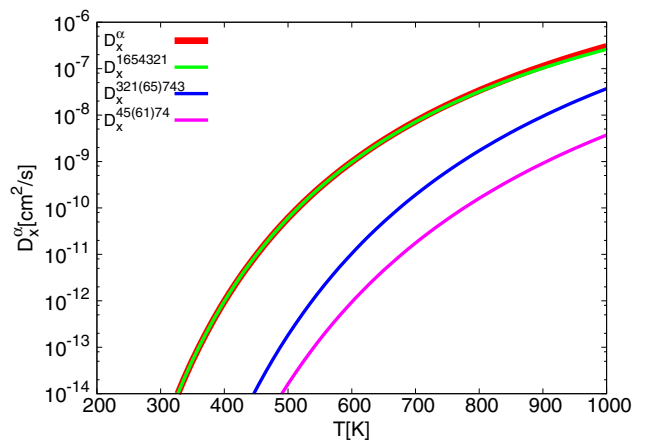

FIG. 12. (Color online) Diffusion coefficient of the Ga adatom in the x direction over the GaAs(001) $(4 \times 4)\alpha$ reconstructed surface.
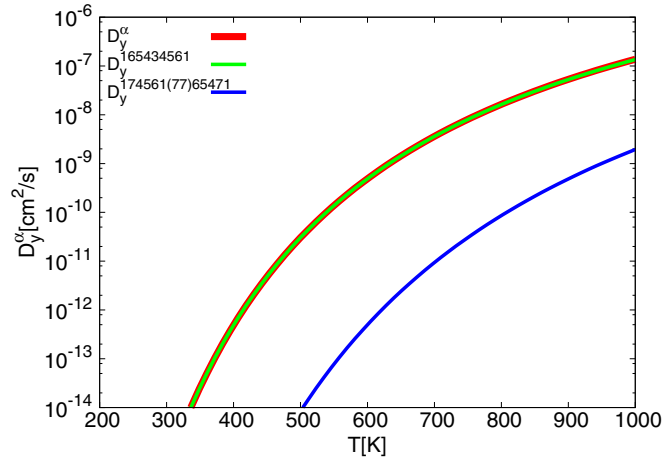
FIG. 13. (Color online) Diffusion coefficient of the Ga adatom in the y direction over the GaAs(001) $(4 \times 4)\alpha$ reconstructed surface.

$\phi_y^3 = \phi_y^1 = 0$ and $\phi_x^a = \phi_x^b$, $\phi_y^a = -\phi_y^b$ for sites 4, 5, 6, and 7. Finally, diffusion coefficients come out as

$$D_x^\alpha = \frac{W_{14} W_{14}' \theta_1 + W_{14} \tilde{W}_{14} P_{eq}^4 + 2 W_{14}' \tilde{W}_{14} \theta_4}{2 W_{14} + W_{14}' + \tilde{W}_{14}} a^2, \quad (20)$$

$$D_y^\alpha = \frac{W_{14} W_{14}'' P_{eq}^1 P_{eq}^1 + W_{14} W_{43} P_{eq}^1 P_{eq}^4}{W_{14} P_{eq}^1 + W_{14}'' P_{eq}^1 + W_{43} P_{eq}^4} a^2, \quad (21)$$

where

$$\frac{1}{W_{14} P_{eq}^1} = \frac{1}{W_{16} P_{eq}^1} + \frac{1}{W_{65} P_{eq}^6} + \frac{1}{W_{54} P_{eq}^5},$$

$$\frac{1}{W_{14}' P_{eq}^1} = \frac{1}{2 W_{17} P_{eq}^1 + 2 W_{57} P_{eq}^5} + \frac{1}{2 W_{74} P_{eq}^7},$$

$$\frac{1}{\tilde{W}_{14} P_{eq}^1} = \frac{1}{2 W_{43} P_{eq}^4} + \frac{1}{W_{32} P_{eq}^3} + \frac{1}{W_{21} P_{eq}^2}, \quad (22)$$

$$\frac{1}{W_{14}'' P_{eq}^1} = \frac{1}{W_{17} P_{eq}^1 + W_{57} P_{eq}^5 + 2 W_{77} P_{eq}^7} + \frac{1}{W_{74} P_{eq}^7}.$$

In the above expression all particle transitions plotted in Fig. 8 were taken into account, but two of them, namely (57) and (17), were approximated by a simple sum as if they both came out from site (1). This is an approximation of very fast jumps between (1) and (5), i.e., much faster than both jumps (57) and (17) which is true in our case. Formulas obtained with this approximation are not far from the exact solution, but they have a simpler structure and give an opportunity to analyze different diffusion paths over the surface. These paths are plotted in Figs. 10 and 11.

It can be seen that there are three possible ways over which a particle diffuses in the x direction and two in the y direction. Their contributions to the global diffusion coefficient are presented in Figs. 12 and 13. The fastest paths in both directions come along the trench and do not climb the hill. Diffusion along axis x happens mainly through two channels—first, the more important one inside the trench, and the second one also visits dimer hills. Both these channels were identified in Ref. [2] on the basis of energy differences for consecutive jumps. The fastest path in the y direction comes
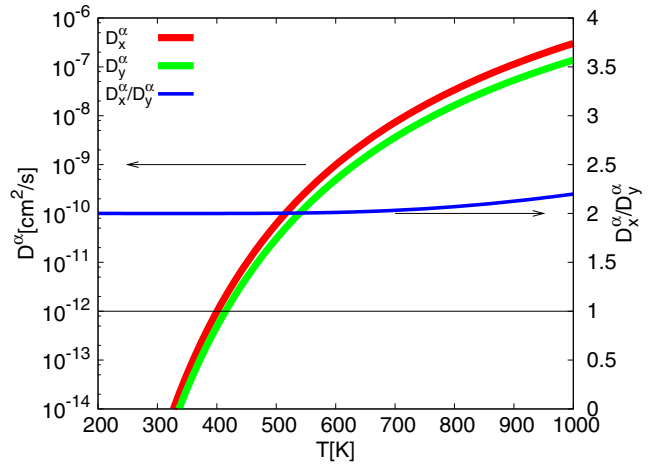

FIG. 14. (Color online) Comparison of diffusion coefficients in the x and y directions for the GaAs(001) $(4 \times 4)\alpha$ reconstructed surface as a temperature function in logarithmic scale. The scale of the anisotropy coefficient is shown on the right.

through sites (16543) and covers almost totally the value of diffusion coefficient D_y. This last diffusion channel was not proposed before as a possible diffusion path [2], whereas it is important and an interesting example of particle way that avoids the lowest energetically site (now it is site 2).

An anisotropy of the particle diffusion at the reconstructed surface $(4 \times 4)\alpha$ is shown in Fig. 14. Within the whole plotted range of temperatures diffusion is larger in the x direction (parallel to dimers) than in the y direction (perpendicular to dimers). The blue dashed line shows ratio between D_x and D_y coefficients. It starts from 2 at low temperature and increases to 2.2 for higher temperatures. Thus comparing these values with those calculated for the surface $(4 \times 4)\beta$ in Fig. 14 we conclude that the diffusion anisotropy is higher at α surface reconstruction. It means that the change of surface symmetry affects the symmetry of the diffusion coefficient of single Ga particles. When we compare activation barriers for diffusion along directions x and y in Fig. 15 we find the same situation as at the previously described surface, namely E_A^x is larger
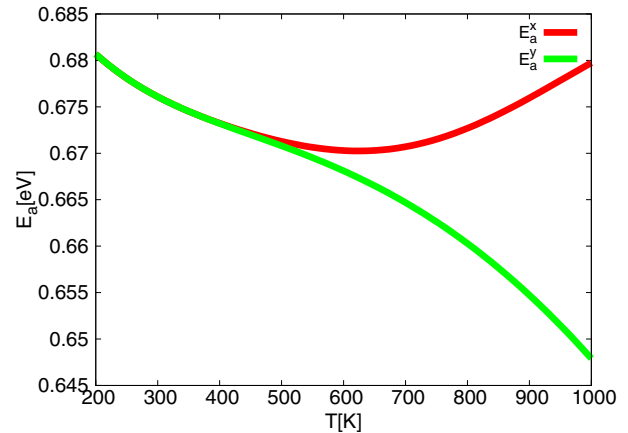

FIG. 15. (Color online) Temperature dependence of the activation energies calculated with use of (18) for total diffusion coefficients D^α in both directions.

than E_A^y. We again can explain this fact through the number of possible diffusion ways. Activation energies compared for diffusion over surfaces α and β are lower for more a complex structure of α symmetry in both directions. We can understand such property as the dependence of the diffusion coefficient on a larger number of transition rates in the α phase. As a result the overall diffusion coefficient has a relatively low activation energy value and a low prefactor ν.

V. CONCLUSIONS

We have calculated diffusion coefficients for two versions of $c(4 \times 4)$ reconstructed surface of GaAs(001) β and α reconstructions. On using a variational formula for the diffusion coefficient we were able to derive a global expression for the elements of the diffusion coefficient tensor on the basis of the derived in *ab initio* calculations energy landscape of adsorption sites and energy barriers [1,2]. In the coordinate system used here our diffusion tensor has only diagonal elements. Diffusion along the direction parallel to the dimer orientation (x) is higher in all cases. However, at low temperatures at the β surface phase diffusion is almost isotropic. The anisotropy increases with temperature and is higher for the α surface phase.

There are not many experimentally measured values of the diffusion coefficient even for the more popular (2×4) GaAs surface reconstruction and there are almost no data for the (4×4) reconstructed surfaces. Yet as it was discussed in Ref. [20] some results from RHEED oscillations allow us to derive a conclusion about rapid enhancement of the diffusion coefficient which can be caused by the change of surface

reconstruction as it was shown in Ref. [47] and which is also qualitatively consistent with the results of our calculations. The value of the diffusion coefficient can be rather compared with the MC data. We have found that our results agree with data from Ref. [32].

The structure of the diffusion coefficient as a sum of different components allows for identification of different diffusion paths. Some of these paths agree with ones guessed from the observation of the energy barrier for successive jumps. The method also allows for finding other paths not so obvious while the energy structure is studied. It appears that α structure is far more asymmetric than β structure. And also when we compare values of coefficients it comes out that diffusion over the surface with lower symmetry $(4 \times 4)\alpha$ is of one order of magnitude lower than that for the surface of $(4 \times 4)\beta$ symmetry. It appears that changes of surface structure towards the system of lower symmetry can be noted in the decrease of the diffusion process. A faster, more effective diffusion process at a given temperature is characteristic for the surface β, the reconstruction of higher symmetry.

A general variational approach that was presented in this work allows for systematic study of the diffusive particle motion. We have shown how it works at surfaces. It can also be easily applied to describe bulk tracer diffusion, more complex phenomena like cluster diffusion, or any other diffusion process for which an appropriate potential energy surface can be determined.

ACKNOWLEDGMENT

[1] J. L. Roehl, A. Kolagatla, V. K. K. Ganguri, S. V. Khare, and R. J. Phaneuf, Phys. Rev. B **82**, 165335 (2010).

[2] J. L. Roehl, S. Aravelli, S. V. Khare, and R. J. Phneuf, Surf. Sci. **606**, 1303 (2012).

[3] J. N. Shapiro, A. Lin, D. L. Huffaker, and C. Ratsch, Phys. Rev. B **84**, 085322 (2011).

[4] W. D. Wheeler, B. A. Parkinson, and Y. Dahnovsky, J. Chem. Phys. **135**, 024702 (2011).

[5] J. Ferron, R. Miranda, and J. J. de Miguel, Phys. Rev B **90**, 125437 (2014).

[6] R. Gonzalez-Hernandez, W. Lopez-Perez, M. G. Moreno-Armenta, and J. A. Rodriguez M, J. Appl. Phys. **110**, 083712 (2011).

[7] S. Booyens, M. Bowker, and D. J. Willock, Surf. Sci. **625**, 69 (2014).

[8] Y.-A. Zhu, D. Chen, X.-G. Zhou, P.-O. Strand, and W.-K. Yuan, Surf. Sci. **604**, 186 (2010).

[9] A. Podsiady-Paszkowska and M. Krawiec, Surf. Sci. **622**, 9 (2014).

[10] F. Liu, W. Hub, Y. Chen, H. Deng, H. Chena, X. Yang, and W. Luod, Surf. Sci. **624**, 89 (2014).

[11] G. Antczak and G. Ehrlich, *Surface Diffusion: Metals, Metal Atoms, and Clusters* (Cambridge University Press, Cambridge, 2010).

[12] G. Antczak, Phys. Rev. B **73**, 033406 (2006).

[13] M. Krawiec and M. Jałochowski, Phys. Rev. B **87**, 075445 (2013).

[14] K. A. Fichthorn, Y. Tiwary, T. Hammerschmidt, P. Kratzer, and M. Scheffler, Phys. Rev. B **83**, 195328 (2011).

[15] A. Kley, P. Ruggerone, and M. Scheffler, Phys. Rev. Lett. **79**, 5278 (1997).

[16] A. Ohtake, Surf. Sci. Rep. **63**, 295 (2008).

[17] V. H. Etgens, M. Sauvage-Simkin, R. Pinchaux, J. Massies, N. Jedrecy, A. Waldhauer, and N. Greiser, Surf. Sci. **320**, 252 (1994).

[18] U. Resch-Esser, N. Esser, D. T. Wang, M. Kuball, J. Zegenhagen, B. O. Fimland, and W. Richter, Surf. Sci. **352–354**, 71 (1996).

[19] A. Nagashima, M. Tazima, A. Nishimura, Y. Takagi, and J. Yoshino, Surf. Sci. **493**, 227 (2001).

[20] T. Ito, K. Tsutsumida, K. Nakamura, Y. Kangawa, K. Shiraishi, A. Taguchi, and H. Kageshima, Appl. Surf. Sci. **237**, 194 (2004).

[21] S. Kaku, J. Nakamura, K. Yagyua, and J. Yoshino, Surf. Sci. **625**, 84 (2014).

[22] A. Nagashima, A. Nishimura, T. Kawakami, and J. Yoshino, Surf. Sci. **564**, 218 (2004).

[23] E. Penev, P. Kratzer, and M. Scheffler, Phys. Rev. Lett. **93**, 146102 (2004).

[24] A. Ohtake, J. Nakamura, S. Tsukamoto, N. Koguchi, and A. Natori, Phys. Rev. Lett. **89**, 206102 (2002).

[25] M. Takahasi and J. Mizuki, Phys. Rev. Lett. **96**, 055506 (2006).

[26] P. Jiříček, M. Cukr, I. Bartoš, and J. Sadowski, Surf. Sci. **603**, 3088 (2009).

[27] A. Ohtake, J. Nakamura, N. Koguchi, and A. Natori, Surf. Sci. **566–568**, 58 (2004).

[28] M. Lòpez and Y. Nomura, J. Cryst. Growth **150**, 68 (1995).

[29] S. Koshiba, Y. Nakamura, M. Tsuchiya, H. Noge, H. Kano, Y. Nagamune, T. Noda, and H. Sakaki, J. Appl. Phys. **76**, 4138 (1994).

[30] T. Shitara, D. D. Vvedensky, M. R. Wilby, J. Zhang, J. H. Neave, and B. A. Joyce, Phys. Rev. B **46**, 6825 (1992).

[31] C. C. Matthai and G. A. Moran, Appl. Surf. Sci. **123-124**, 653 (1998).

[32] J. G. LePage, M. Alouani, D. L. Dorsey, J. W. Wilkins, and P. E. Blöchl, Phys. Rev. B **58**, 1499 (1998).

[33] M. Rosini, M. C. Righi, P. Kratzer, and R. Magri, Phys. Rev. B **79**, 075302 (2009).

[34] F. Montalenti and R. Ferrando, Phys Rev Lett. **82**, 1498 (1999).

[35] T. Ala-Nissila, R. Ferrando, and S. C. Ying, Adv. Phys. **51**, 949 (2002).

[36] J. W. Haus and K. W. Kehr, Phys. Rep. **150**, 263 (1987).

[37] E. Penev, P. Kratzer, and M. Scheffler, Phys. Rev. B **64**, 085401 (2001).

[38] E. Penev, S. Stojkovic, P. Kratzer, and M. Scheffler, Phys. Rev. B **69**, 115335 (2004).

[39] Z. W. Gortel and M. A. Załuska-Kotur, Phys. Rev. B **70**, 125431 (2004).

[40] M. A. Załuska-Kotur and Z. W. Gortel, Phys. Rev. B **72**, 235425 (2005).

[41] Ł. Badowski, M. A. Załuska-Kotur, and Z. W. Gortel, Phys. Rev. B **72**, 245413 (2005).

[42] M. A. Załuska-Kotur and Z. W. Gortel, Phys. Rev. B **74**, 045405 (2006).

[43] Ł. Badowski, M. A. Załuska-Kotur, and Z. W. Gortel, J. Stat. Mech. (2010) P03008.

[44] K. Morgenstern, K.-F. Braun, and K.-H. Rieder, Phys. Rev. Lett. **93**, 056102 (2004).

[45] J. L. Roehl and S. V. Khare, Solar Energy **101**, 245 (2014).

[46] J. L. Roehl and S. V. Khare, Solar Energy Mater. Solar Cells **128**, 343 (2014).

[47] A. Shen, Y. Horikoshi, H. Ohno, and S. P. Guo, Appl. Phys. Lett. **71**, 1540 (1997).

[48] R. Gomer, Rep. Prog. Phys. **53**, 917 (1990).

[49] P. Pechukas, in *Dynamics of Molecular Collisions: Part B*, edited by W. H. Miller (Plenum, New York, 1976).

[50] V. P. LaBella, D. W. Bullock, C. Emery, Z. Ding, and P. M. Thibado, Appl. Phys. Lett. **79**, 3065 (2001)

[51] U. Kürpick, A. Kara, and T. S. Rahman, Phys. Rev. Lett. **78**, 1086 (1997).

[52] J. Schnakenberg, Rev. Mod. Phys. **48**, 571 (1976).